Dewetting-Induced Membrane Formation by Adhesion of Amphiphile-Laden Interfaces

Ho Cheung Shum,[†,‡] Enric Santanach-Carreras,[§,¶] Jin-Woong Kim,[∥] Allen Ehrlicher,[†] Jerome Bibette,[§] and David A. Weitz*[,†,⊥,#]

[†]School of Engineering and Applied Sciences, and Harvard University, Cambridge, Massachusetts 02138, United States

[‡]Department of Mechanical Engineering, University of Hong Kong, Pokfulam Road, Hong Kong

[§]ESPCI ParisTech, LCMD, UPMC Université Paris 06, UMR 7195, 10 rue Vauquelin, 75231 Paris, France

[¶]Capsum, 3 Allee des maraichers, Heliopolis, 13013 Marseille, France

[∥]Department of Applied Chemistry, Hanyang University, 1271, Sa3-dong, Sangnok-gu, Ansan-si, Gyeonggi-do 426-791, Korea

[⊥]Department of Physics, Harvard University, Cambridge, Massachusetts 02138, United States

[#]Kavli Institute for Bionano Science and Technology, Harvard University, Cambridge, Massachusetts 02138, United States

S *Supporting Information*

ABSTRACT: We introduce an approach for forming bilayer polymer membranes by adhesion of amphiphile-laden interfaces. This adhesion is induced by a reduction of solvent quality for the amphiphilic diblock copolymers through selective evaporation of good solvent in the solvent mixture. By combining this membrane formation mechanism with a double-emulsion-templated approach for vesicle formation, we fabricate monodisperse polymersomes that exhibit excellent membrane uniformity, and structural stability, using a method that has high encapsulation efficiency. Moreover, we also show that the technique is versatile and can be applied to different block copolymers. The ability to direct the assembly of amphiphiles into a membrane creates new opportunities to engineer the structures of vesicles on the level of the individual bilayer leaflets.
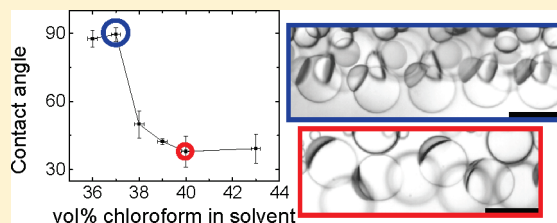
INTRODUCTION

Amphiphilic molecules such as surfactants, lipids, and polymers can serve as building blocks for more complicated structures; examples of such structures include liposomes and polymersomes, which are bilayer structures that can enclose aqueous materials in water and can be artificial analogues of cell membranes. These structures have great promise as delivery vehicles for drugs and enzymes and as bioreactors for biomedical applications; they also have great potential as a key component of artificial cells. Polymersomes are of particular interest due to their enhanced stability and low permeability to encapsulants, as compared to liposomes. In addition, the versatility of synthetic polymer chemistry enables manipulation of membrane thickness, surface functionality, degradation kinetics of polymersomes,[1,2] and incorporation of functional species inside the membrane,[3] making them a highly tunable structure for encapsulation and release of actives. For example, by linking cell-penetrating peptides to the block copolymers, enzyme-loaded polymersomes can enter cells and induce intracellular catalysis.[4] Typically, polymersomes are self-assembled;[5−8] for instance, with techniques such as hydration and electroformation, preformed planar lipid membranes self-assemble into vesicles under mechanical and electrical agitation in water. However, the underlying principles of this self-assembly are still not fully understood. This lack of understanding challenges our ability to form highly controlled vesicles and can hinder our ability to design artificial membranes that would lead to useful applications in fields as varied as cosmetics, drug delivery, and bioreactors.

To overcome the limitations of self-assembly of these structures, the controlled flow of microfluidics has been used for their fabrication. One strategy to form these vesicles is to induce nucleation of polymersomes by mixing a polymer-containing solvent stream with a nonsolvent in a microfluidic device using a flow-focusing geometry; this results in the formation of polymersomes whose size can be tuned by varying the flow rates of the fluids.[9] This approach has also been used for fabricating liposomes,[10,11] liposome−hydrogel hybrid nanoparticles,[12] and vesicles of nonionic surfactants.[13] However, since the fluid phase containing the actives and the polymers is miscible with the nonsolvent phase, some actives are released to the continuous phase during mixing; as a result, the encapsulation efficiency of this approach is limited. Another strategy is to shear a preformed lipid membrane to form vesicles by microfluidic flow.[14−16] With this approach, the bilayer membrane is fully formed before being configured into a vesicle structure. A third strategy is to use controlled double-emulsion droplets prepared in microfluidic devices as templates for forming polymersomes. Double emulsions can be generated in microfluidic devices where the

active-containing phase is completely separated from the outermost continuous phase by an oil shell;[17] thus, these double-emulsion-templated polymersomes can achieve almost 100% encapsulation efficiency.[18] A similar strategy has also been applied to form phospholipid vesicles.[19] In the double-emulsion-templated approach, the overall structure of the vesicles is formed using a core—shell structure; however, the bilayer membranes must then be assembled within this shell. Therefore, a thorough understanding of the assembly of diblock copolymers into bilayer membranes is particularly crucial for the formation of polymersomes using the double-emulsion-templated approach.

During the conversion of double-emulsion drops to polymersomes, a dewetting transition is observed, as the shell solvents evaporate; the shell phase dewets at the interface of the innermost drop and collects on one side of the inner drop, forming an acornlike shape.[18,20] The shell phase remains attached to the drops and must be removed by evaporation, which can take up to several days. The acornlike geometry of the dewetted drops implies there is adhesion between the inner and outer interfaces of the shell.[21] In water-in-oil emulsions (W/O), such adhesion has been observed when the oil phase consists of two different oils, one in which the surfactant is soluble and the other in which the surfactant is insoluble.[22] The adhesion between the surfactant monolayers varies strongly as a function of the composition of the oil mixture. Although this mechanism has been used to induce aggregation of emulsions, its applicability for making bilayer vesicles has not been demonstrated. A better understanding is needed for designing more controlled vesicles and for establishing criteria for controlled fabrication of polymersomes. This will extend the applicability of this double-emulsion-templated approach to a wider range of polymers for specific functions and properties of the resultant polymersomes.[23,24]

In this work, we study the formation of polymer membranes as a function of the composition of the solvent mixture using water-in-oil-in-water (W/O/W) double emulsions prepared by capillary microfluidics. By employing a mixture of a volatile good solvent and a less volatile poor solvent for an amphiphilic diblock copolymer as the oil phase of the double emulsions, we elucidate the mechanism behind the formation of polymersomes induced by a dewetting transition. As the fraction of good solvent is reduced by evaporation, the adhesion between the amphiphilic diblock copolymer monolayers at the two interfaces becomes stronger. This new understanding enables an efficient process for polymersome fabrication without the requirement of a subsequent step to evaporate the solvents. We show that the resultant polymersomes encapsulate both hydrophilic and hydrophobic actives. In addition, from fluorescence recovery after photobleaching (FRAP) measurements, the polymersome membranes exhibit slow diffusion kinetics as compared to phospholipid vesicles. Under osmotic pressure, the polymersomes also exhibit buckling behavior that reflects the rigid amorphous nature of membranes. Our approach provides a robust and general method to create monodisperse rigid polymersomes with precisely tuned structures and excellent encapsulation properties.

■ RESULTS AND DISCUSSION

As templates for the polymersomes, W/O/W double-emulsion drops with an oil shell of a diblock copolymer, poly(ethylene glycol)-b-poly(lactic acid) [PEG(5000)-b-PLA(5000)], dissolved in a mixture of chloroform and hexane were generated using a glass capillary microfluidic device that combines a coflow
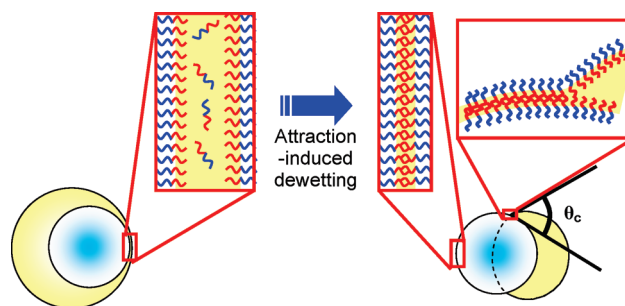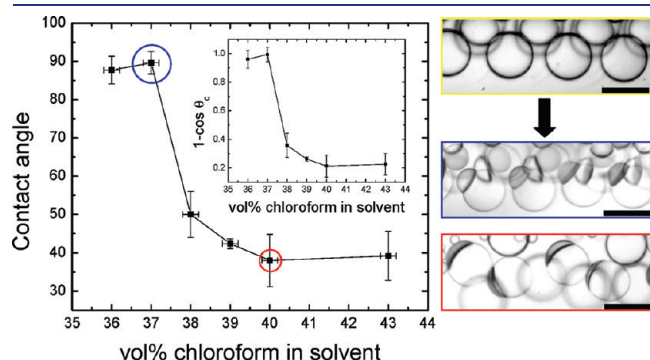

Figure 1. Schematic of the dewetting transition induced by the attraction of the two interfaces of the double-emulsion drops.

and a flow-focusing geometry (see the Supporting Information, Figure S1).[25] The amphiphilic diblock copolymers adsorb at the inner—middle and the middle—outer interfaces, with the hydrophobic blocks of PLA in the solvent phase and the hydrophilic blocks of PEG in the inner phase and the continuous phase; thus, the double-emulsion drops are stabilized. These emulsions undergo a transition from complete wetting to partial wetting of the middle phase.[18,20] From a simple force balance, this implies a negative spreading coefficient, $S = \gamma_{IO} - \gamma_{IM} - \gamma_{MO} < 0$, where γ_{IO}, γ_{IM}, and γ_{MO} are the interfacial tensions of the inner—outer, the inner—middle, and the middle—outer interfaces.[18] The spreading coefficient is a good indicator that predicts whether dewetting transition will occur, but it does not provide any physical insights on how dewetting can be induced. A negative spreading coefficient is associated with an attractive adhesion energy between the inner—middle and middle—outer interfaces. In this work, we manipulate this adhesion to induce dewetting and formation of bilayer membranes by using a mixture of a more volatile good solvent and a less volatile poor solvent for the diblock copolymers. Since the solubility of chloroform in water (~8 g/L at 20 °C) is significantly higher than that of hexane (~13 mg/L at 20 °C), chloroform in the oil shell diffuses into the continuous phase and is evaporated at a much faster rate than hexane. The solvent mixture becomes increasingly hexane-rich, turning into a poor solvent for the diblocks, which start to precipitate in bulk. When the diblock copolymers are confined to the two proximal interfaces of the core—shell double-emulsion drop, the reduction in solvent quality of the shell phase leads to attraction between the PLA blocks, triggering a dewetting transition, with the diblock copolymers at the two interfaces sticking to one another, forming a membrane and expelling the solvent, as illustrated schematically in Figure 1. The remaining solvent forms a droplet on the membrane formed. The contact angle, θ_c, at the three-phase contact point is related to the strength of the adhesion between the two copolymer monolayers at the interfaces.

To characterize this phenomenon, we measure the contact angle as a function of the volume fraction of chloroform in the solvent mixture that forms the shell phase of the double-emulsion templates, as plotted in Figure 2. Before dewetting occurs, the shell phase wets the inner drops completely, as shown by the core—shell structures of the double-emulsion drops in the image surrounded by the yellow box in Figure 2. When the drops flow downstream, chloroform in the shell phase starts to diffuse into the continuous phase. This induces dewetting of the shell phase on the surface of the inner drops, and the contact angle at which the dewetted shell phase is attached to the vesicles depends critically on the starting composition of the shell phase. As the
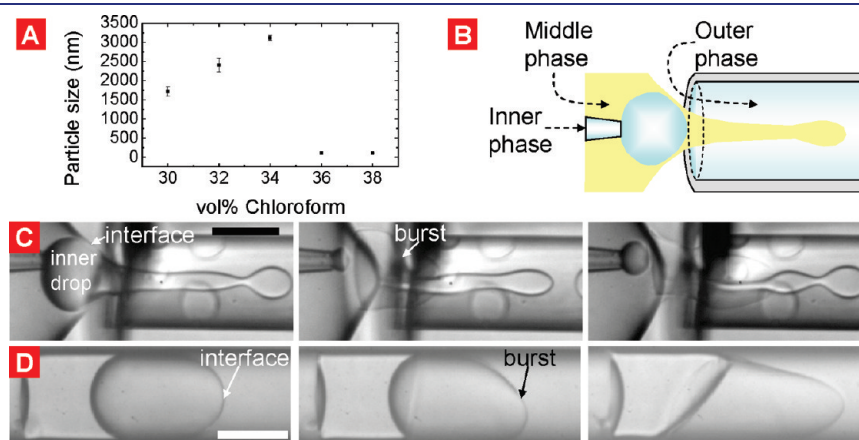
fraction of chloroform is decreased from 43 to 38 vol%, the contact angle increases slowly from about 40° to 50°, as shown in Figure 2. The contact angle increases significantly to about 90° at chloroform volume fraction of 37 vol%. On the basis of the Young–Dupré equation, $\Delta F = 2\gamma(1 - \cos\theta_c)$, where γ is the interfacial tension between the aqueous phase and the solvent phase, the energy of adhesion, ΔF, can be deduced. The energy of adhesion is highest at chloroform volume fraction of 36–37 vol% and decreases as the fraction of chloroform increases, as shown in the inset in Figure 2. This agrees with the trend for the solubility of the diblock copolymers in the solvent mixture, which is the

origin of the adhesion. The results also suggest the existence of two membrane states depending on the strength of the attractive interactions during the assembly of the amphiphiles. At low chloroform fractions of 36–37 vol%, which correspond to a strong adhesion between the copolymer monolayers, the copolymers are insoluble in the solvent mixture and it is highly unfavorable for any solvent to be trapped between the monolayers. However, at lower chloroform fraction, the energetic penalty for solvent to be trapped between the two layers is lowered. The presence of these two membranes states may explain the jump in the contact angle shown in Figure 2.

According to the relationship between adhesion strength and fraction of chloroform, reducing the chloroform fraction should favor formation of polymersomes. However, experimentally, as the volume fraction of chloroform is reduced to below 35 vol%, no polymersomes are formed. In a solvent mixture with such a low chloroform fraction, the diblock copolymer is essentially insoluble and starts to precipitate. We measure the initiation of copolymer precipitation using dynamic light scattering by adding hexane to chloroform with diblock copolymers dissolved to make up solvent mixtures with varying fraction of chloroform while keeping PEG(5000)-*b*-PLA(5000) concentration to 10 mg/mL. Large aggregates with sizes above 1 μm can be observed in the solvent mixture as the chloroform fraction is at or below 34 vol%, as shown in Figure 3A. When double emulsions are generated using solvent mixtures with such low chloroform fraction as the shell phase, the resultant double-emulsion drops are unstable. We demonstrate this using a glass capillary device with an untapered collection tube, as shown in Figure 3B. An untapered collection tube is used here instead of a tapered one to avoid having multiple double-emulsion drops in the field of view; this occurs in an untapered collection tube due to the slowing of the flow as the channel widens. At the tip of the injection capillary, the inner drops of the double-emulsion drops coalesce with the continuous phase before generation, as shown in Figure 3C. The amphiphilic diblock copolymer molecules do not stabilize the thin interface sufficiently to prevent the inner drops from bursting into the

Figure 2. Plot of the contact angle (θ_c) of the solvent drops on the vesicles as a function of the fraction of the solvent, chloroform. The volume fraction of chloroform is determined before injection of the solvent mixture into the device; the exact composition during dewetting may vary slightly due to diffusion into the aqueous phases. In all the experiments, dewetting occurs inside the capillary microfluidic devices within seconds of generation of the double emulsions; thus, all the angles are measured with little time for the solvents to fully equilibrate with the surrounding liquid phases. The images in the yellow, blue, and red boxes show optical microscopy images of the drops before dewetting, dewetted drops at 36 vol % chloroform, and dewetted drops at 39 vol % chloroform, respectively. Scale bars are 50 μm. The inset shows a plot of $1 - \cos\theta_c$ as a function of the fraction of chloroform.

Figure 3. (A) Size of the aggregates as a function of the volume fraction of chloroform in the solvent mixture. (B) Illustration of the geometry of the microchannel for studying the stability of the double emulsions generated. (C) Series of optical microscope images showing the coalescence of the inner droplet with the outer phase before generation of a double-emulsion drop. "Burst" refers to the process of coalescence between the inner drop and the outer continuous phase. Due to the slight difference in the refractive indexes of the two phases, a halo around the original inner droplet phase can still be observed shortly after the coalescence. The solvent mixture in the middle phase contains 10 mg/mL PEG(5000)-*b*-PLA(5000) in 30 vol% chloroform and 70 vol% hexane. The time interval between successive images is 1 ms, and the scale bar is 50 μm. (D) Series of optical microscope images showing the destabilization of the double-emulsion drop in the microchannel. The solvent mixture contains 10 mg/mL PEG(5000)-*b*-PLA(5000) in 50 vol% chloroform and 50 vol% hexane. The time interval between successive images is 1.5 ms, and the scale bar is 50 μm.

4422

dx.doi.org/10.1021/ja108673h | *J. Am. Chem. Soc.* 2011, 133, 4420–4426
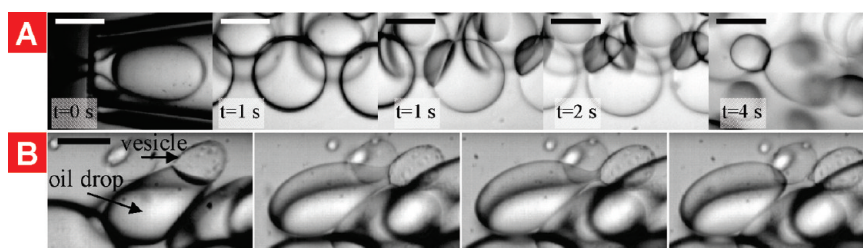
Figure 4. Microfluidic fabrication of polymersomes in a microchannel. (A) Series of optical micrographs showing the generation of a double-emulsion drop and the subsequent dewetting transition. Scale bars are 50 μm. (B) Series of optical micrographs showing the separation of the polymersome from the oil drop by the shear in the microchannel. The time interval between successive images is 10 ms, and the scale bar is 50 μm.

continuous phase; even when the double-emulsion drops are formed, coalescence occurs in the microchannel soon after generation. We attribute this to the precipitation of the diblock copolymers at chloroform fractions below 35 vol%; this depletes the solvent mixture of sufficient amphiphilic copolymers for stabilizing the double emulsion. However, when the chloroform fraction is above 43 vol%, the double-emulsion drops are also unstable and no dewetting is observed. The inner drops of the double emulsion formed eventually burst and coalesce with the continuous phase, as shown in Figure 3D. We believe that, in this case, the diblock copolymers are solvated in the solvent mixture and the copolymer molecules at the interfaces are in dynamic equilibrium with the bulk shell phase. Since there is no driving force for precipitation, the two interfaces are not attracted to each other, and thus no dewetting occurs.

Our results indicate that the dewetting-induced transition from double emulsions to polymersomes occurs most readily within a certain range of ratio of good solvent to poor solvents in the solvent mixture forming the shell phase of the double emulsions. When the ratio is too low, the block copolymers can hardly dissolve in the solvent mixture; when the ratio is too high, adhesion between the monolayers is too small. The behavior is general and can be applied to different solvent conditions and different block copolymers (see Figure S2 in the Supporting Information). In the case of PEG(5000)-*b*-PLA(5000) with chloroform and hexane as the good and poor solvents, respectively, dewetting occurs most readily with the highest adhesion between the copolymer monolayers when the fractions of chloroform and hexane in the shell phase of the double-emulsion templates are 36 and 64 vol%, respectively. Such double-emulsion droplets start to dewet and form acornlike geometry within 1−2 s after generation in the capillary device, as shown in the series of images in Figure 4A. We also demonstrate similar dewetting of a double-emulsion droplet inside an untapered collection capillary in Supporting Information Figure S3A. When the flow rate of the shell phase is reduced and the resultant shell becomes sufficiently thin, dewetting can occur during droplet generation. Understanding of the mechanism that triggers dewetting enables the optimization of the solvent mixture for dewetting and allows minimization of the time needed to trigger dewetting.

Under optimal conditions, dewetting can be induced to occur inside the device, representing a significant improvement from previous techniques.[18] For the diblock copolymer PEG(5000)-*b*-PLA(5000), optimal volume fractions of chloroform and hexane are 36 and 64 vol %, respectively, as confirmed after repeated characterization. With this solvent mixture, the dewetting transition is completed inside the device; the remaining solvent droplets can be sheared off from the polymersomes by flow inside the microfluidic channel, as shown in the series of images

in Figure 4B. The shearing off can occur at slightly different distances from the tip where double-emulsion drops are generated. The yield of the shearing off can be improved by increasing the distance traveled by the polymersomes before collection; this ensures that the solvent droplets are sheared off of all the polymersomes. Similar droplet detachment can be observed in an untapered channel, as shown in Supporting Information Figure S3B. As a result of these improvements, complete evaporation of the solvent that contains excess diblock copolymers is no longer needed. Almost all of the solvent, with the excess diblock copolymers, can be removed by shearing due to microfluidic flow; trace amounts of residual solvent trapped between the membranes are removed spontaneously through evaporation. Thus, this new approach is significantly less time-consuming, and the polymersomes can now be collected directly from the product stream coming out of the microfluidic device. Moreover, the resultant polymersomes have homogeneous membranes with even thicknesses across the whole surface of the polymersomes. The size distribution of the polymersomes is determined by that of the inner droplets of the double-emulsion templates; thus, they are highly monodisperse. Although, in principle, the size distribution of the inner droplets is independent of the solvent composition of the middle phase, stability of the double emulsions limits the range of solvent compositions at which polymersomes can be prepared.

For practical applications of the polymersomes, an ability to adjust the volume fraction of the polymersomes is desirable. To increase the density of the polymersomes and promote sedimentation in the collection vials, we encapsulate a 10 wt % poly(ethylene glycol) with an average molecular weight of 6000 Da [PEG(6000)] inside the polymersomes. The polymersomes are then collected in a sodium chloride solution with the same osmolality ($\sim$100 mOsm) as the PEG(6000) solution. This results in a concentrated suspension of polymersomes. The concept demonstrated in this work does not rely on the presence of the PEG(6000), which is added only to increase the density, thereby increasing the concentration of polymersomes in the final suspension. These polymersomes demonstrate excellent encapsulation efficiency, as shown by the encapsulation of a hydrophilic fluorescent dye, 8-hydroxypyrene-1,3,6-trisulfonic acid trisodium salt (HPTS), with no observable leakage in Figure 5A. The fluorescence drops sharply at the edge of the polymersome, suggesting that virtually all fluorescent dye is encapsulated inside the polymersome, as shown in Supporting Information Figure S4. Current use of the technique in applications that require encapsulation of active ingredients with high efficiency and stability confirms the utility of these polymersomes. In addition, the walls of these polymersomes are also very thin and homogeneous in thickness, as shown by the thin circular outline in the cryogenic

4423

dx.doi.org/10.1021/ja108673h |*J. Am. Chem. Soc.* 2011, 133, 4420–4426
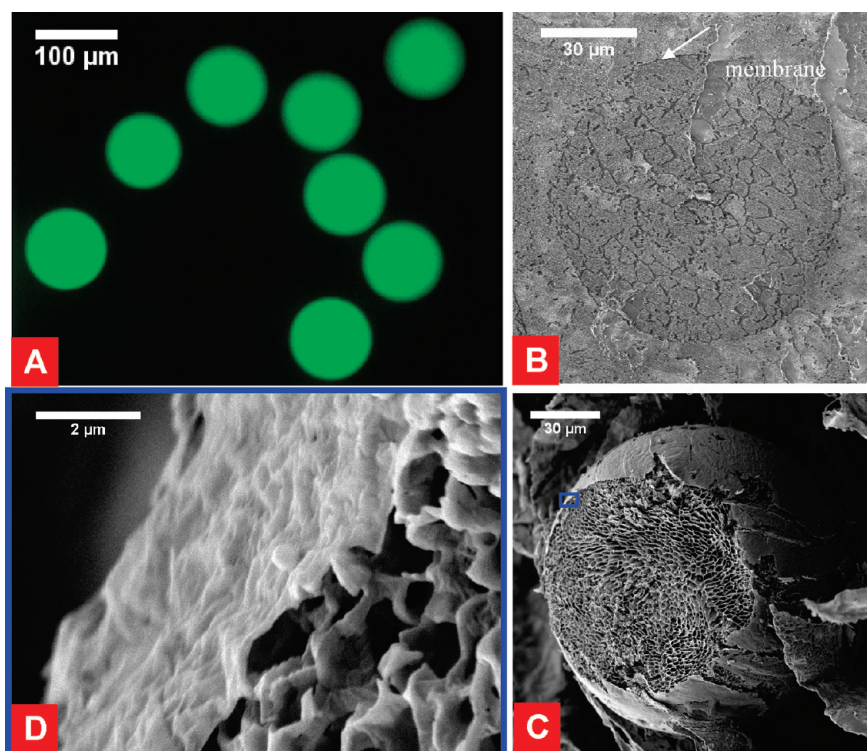
Figure 5. (A) Confocal laser scanning microscope image of PEG(5000)-*b*-PLA(5000) polymersomes encapsulating a fluorescent dye (HPTS). (B) Cryo-scanning electron microscope (cryo-SEM) image of a PEG(5000)-*b*-PLA(5000) polymersome. (C) Scanning electron microscope (SEM) image of a freeze-dried PEG(5000)-*b*-PLA(5000) encapsulating a PEG solution. (D) Magnified view of the region in blue in panel C.
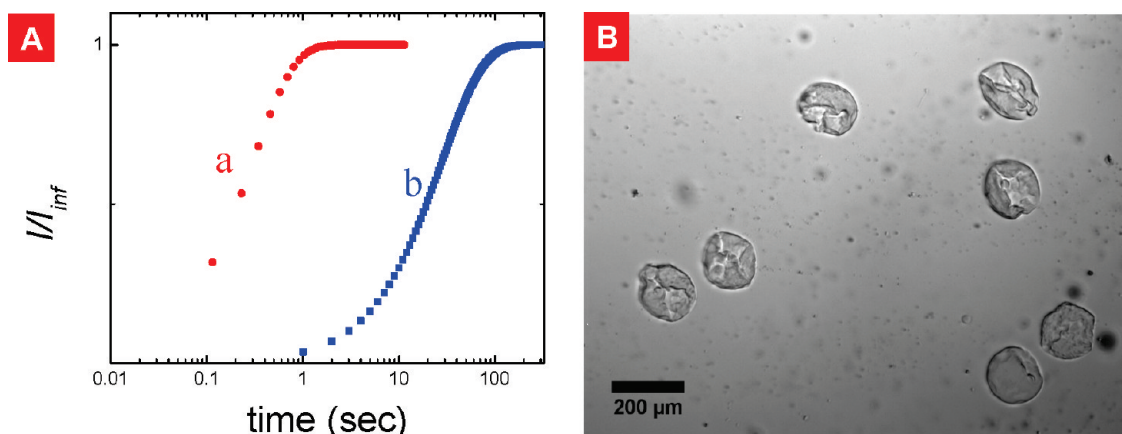
Figure 6. (A) Fluorescence recovery after photobleaching (FRAP) of NBD−norcholesterol in the membranes of (a) an electroformed DOPC vesicle and (b) a double-emulsion-templated PEG(5000)-*b*-PLA(5000) polymersome. The recovery times for curves a and b are 0.37 and 28 s, respectively. I_{inf} refers to the intensity of the NBC−cholesterol within the membranes at $t = \infty$. (B) Optical microscope image of polymersomes crushed in a concentrated solution of PEG with an average molecular weight of 6000 Da. The osmotic pressure exerted on the membrane is about 20 atm.

scanning electron microscope (cryo-SEM) image in Figure 5B. To demonstrate the solidlike nature of the polymersome membrane, suspensions of polymersomes are freeze-dried and imaged with SEM. The dried polymersomes contain thin walls, which are slightly broken, probably due to drying. The excellent encapsulation is highlighted by the containment of a foamlike structure that is typical of dried PEG solution inside the thin polymersome walls, as shown in Figure 5, parts C and D. This indicates that, in the presence of the encapsulated PEG solution, the membranes of the polymersomes are sturdy enough to not disintegrate or rearrange during freeze-drying.

We attribute the surprising rigidity of our polymersomes to the strong adhesion of the diblock copolymer monolayers during dewetting, which we hypothesize to form a gel-like or even glassy layer, imparting additional structural stability to the resultant membrane. To demonstrate the jammed nature of the membrane, we add fluorescent cholesterol as a tracer in the shell phase of our double-emulsion templates, thus forming polymersomes with fluorescent cholesterol inside the membranes for characterization using FRAP. During the measurement, a small spot of the membrane is photobleached completely, and the fluorescence recovers as unbleached fluorescent marker diffuses into the

photobleached region. Therefore, the recovery time is a good measure of the diffusivity of the fluorescent tracer in the membrane. In our experiments, the fluorescence in the membranes of PEG(5000)-*b*-PLA(5000) polymersomes formed with our approach recovers much more slowly than that for electroformed 1,2-dioleoyl-*sn*-glycero-3-phosphocholine (DOPC) vesicles, as shown in Figure 6. The recovery time of about 28 s recorded for the polymersomes is about 2 orders of magnitude slower than that (0.37 s) for the electroformed DOPC vesicles that are known to have fluid membranes. Clearly, diffusion of the fluorescent cholesterol is significantly slowed down in the polymersome membranes. Moreover, we have also applied high osmotic pressure to the polymersomes by introducing PEG at high concentrations to the continuous phase. Unlike liposomes with fluid membranes, which shrink and split into smaller liposomes while maintaining their spherical geometry, the membranes of the polymersomes buckle under high osmotic pressure, as shown in Figure 6B. Similar buckling behavior is also observed after replacing the PEG solution in the inner phase of the polymersomes with a sucrose solution to match osmolality, as shown in Supporting Information Figure S5. The slower recovery time and buckling behavior under applied osmotic pressure for the polymersomes support our hypothesis that the polymersome membranes consist of a gel-like or glassy network, which makes the membranes more rigid and less accessible for the diffusion of small molecules. In this work, we demonstrate the physicochemical concept of using dewetting to induce membrane formation by using emulsion templates of about 100 μm in diameter; these are easier to prepare and visualize than smaller emulsion droplets. However, the concept demonstrated in this work can also be readily applied to make smaller polymersomes, for example, by shrinking the inner droplets of the double-emulsion templates osmotically.

CONCLUSIONS

In this work, we have demonstrated that formation of polymersomes from double-emulsion templates can be achieved by using a mixture of a volatile good solvent and a less volatile poor solvent for dissolving the diblock copolymers in the shell of the templates. By varying the ratio of the solvents, the adhesion between monolayers of block copolymers at the interfaces of the double-emulsion drops is also varied. This is in agreement with the phenomenological rules observed in adhesive single emulsions.[22,26,27] Our results also suggest that formation of membranes with a gel phase is associated with the attraction between the constituent diblock copolymer molecules. This approach provides a general and robust process to continuously generate monodisperse polymersomes that exhibit excellent membrane uniformity, encapsulation efficiency, and structural stability. It also provides a prescription for the choice of polymers and solvents in creating vesicles from different materials. The ability to manipulate mobile amphiphiles before membrane formation creates new opportunities to engineer the vesicle structure on the level of the individual leaflets that make up the bilayer. This would facilitate fabrication of complex structures including multicompartment[28] and asymmetric vesicles.

ASSOCIATED CONTENT

S **Supporting Information.** Experimental section, schematic of the glass capillary microfluidic device for making the

double emulsion, images of polymersomes prepared with different diblock copolymers and solvents, as well as two series of images showing dewetting of double-emulsion drops and subsequent detachment of the solvent drops from the polymersomes inside a microfluidic channel. This material is available free of charge via the Internet at http://pubs.acs.org.

AUTHOR INFORMATION

Corresponding Author
weitz@seas.harvard.edu

ACKNOWLEDGMENT

REFERENCES

(1) Discher, B. M.; Won, Y. Y.; Ege, D. S.; Lee, J. C. M.; Bates, F. S.; Discher, D. E.; Hammer, D. A. *Science* **1999**, *284*, 1143.

(2) Discher, D. E.; Eisenberg, A. *Science* **2002**, *297*, 967.

(3) Mai, Y.; Eisenberg, A. *J. Am. Chem. Soc.* **2010**, *132*, 10078.

(4) van Dongen, S. F. M.; Verdurmen, W. P. R.; Peters, R. J. R. W.; Nolte, R. J. M.; Brock, R.; van Hest, J. C. M. *Angew. Chem., Int. Ed.* **2010**, *49*, 7213.

(5) Shen, H. W.; Eisenberg, A. *Macromolecules* **2000**, *33*, 2561.

(6) Shen, H. W.; Eisenberg, A. *J. Phys. Chem. B* **1999**, *103*, 9473.

(7) Antonietti, M.; Forster, S. *Adv. Mater.* **2003**, *15*, 1323.

(8) Kukula, H.; Schlaad, H.; Antonietti, M.; Forster, S. *J. Am. Chem. Soc.* **2002**, *124*, 1658.

(9) Thiele, J.; Steinhauser, D.; Pfohl, T.; Forster, S. *Langmuir* **2010**, *26*, 6860.

(10) Jahn, A.; Stavis, S. M.; Hong, J. S.; Vreeland, W. N.; DeVoe, D. L.; Gaitan, M. *ACS Nano* **2010**, *4*, 2077.

(11) Jahn, A.; Vreeland, W. N.; DeVoe, D. L.; Locascio, L. E.; Gaitan, M. *Langmuir* **2007**, *23*, 6289.

(12) Hong, J. S.; Stavis, S. M.; Lacerda, S. H. D.; Locascio, L. E.; Raghavan, S. R.; Gaitan, M. *Langmuir* **2010**, *26*, 11581.

(13) Lo, C. T.; Jahn, A.; Locascio, L. E.; Vreeland, W. N. *Langmuir* **2010**, *26*, 8559.

(14) Stachowiak, J. C.; Richmond, D. L.; Li, T. H.; Brochard-Wyart, F.; Fletcher, D. A. *Lab Chip* **2009**, *9*, 2003.

(15) Stachowiak, J. C.; Richmond, D. L.; Li, T. H.; Liu, A. P.; Parekh, S. H.; Fletcher, D. A. *Proc. Natl. Acad. Sci. U.S.A.* **2008**, *105*, 4697.

(16) Ota, S.; Yoshizawa, S.; Takeuchi, S. *Angew. Chem., Int. Ed.* **2009**, *48*, 6533.

(17) Shah, R. K.; Shum, H. C.; Rowat, A. C.; Lee, D.; Agresti, J. J.; Utada, A. S.; Chu, L. Y.; Kim, J. W.; Fernandez-Nieves, A.; Martinez, C. J.; Weitz, D. A. *Mater. Today* **2008**, *11*, 18.

(18) Shum, H. C.; Kim, J. W.; Weitz, D. A. *J. Am. Chem. Soc.* **2008**, *130*, 9543.

(19) Shum, H. C.; Lee, D.; Yoon, I.; Kodger, T.; Weitz, D. A. *Langmuir* **2008**, *24*, 7651.

(20) Hayward, R. C.; Utada, A. S.; Dan, N.; Weitz, D. A. *Langmuir* **2006**, *22*, 4457.

(21) Aronson, M. P.; Princen, H. M. *Nature* **1980**, *286*, 370.

(22) Poulin, P.; Bibette, J. *Langmuir* **1998**, *14*, 6341.

(23) Li, M. H.; Keller, P. *Soft Matter* **2009**, *5*, 927.

(24) Brown, L.; McArthur, S. L.; Wright, P. C.; Lewis, A.; Battaglia, G. *Lab Chip* **2010**, *10*, 1922.

(25) Utada, A. S.; Lorenceau, E.; Link, D. R.; Kaplan, P. D.; Stone, H. A.; Weitz, D. A. *Science* **2005**, *308*, 537.

(26) Bibette, J.; Mason, T. G.; Hu, G.; Weitz, D. A.; Poulin, P. *Langmuir* **1993**, *9*, 3352.

(27) Poulin, P.; Bibette, J. *Langmuir* **1999**, *15*, 4731.

(28) Shum, H. C.; Zhao, Y.-j.; Kim, S.-H.; Weitz, D. A. *Angew. Chem., Int. Ed.* 2011, *50*, 1648.